



Biopolymer-assisted self-assembly of ZnO nanoarchitectures from nanorods

O. Lupan^{a,b,*}, L. Chow^b, G. Chai^c, A. Schulte^b, S. Park^b,
O. Lopatiuk-Tirpak^b, L. Chernyak^b, H. Heinrich^{b,d,e}

^a *Department of Microelectronics and Semiconductor Devices, Technical University of Moldova, 168 Stefan cel Mare Blvd., Chisinau, MD-2004, Republic of Moldova*

^b *Department of Physics, University of Central Florida, Orlando, FL 32816-2385, USA*

^c *Apollo Technologies, Inc., 205 Waymont Court, S111, Lake Mary, FL 32746, USA*

^d *Advanced Materials Processing and Analysis Center, University of Central Florida, Orlando, FL 32816, USA*

^e *Department of Mechanical, Materials, and Aerospace Engineering, University of Central Florida, Orlando, FL 32816, USA*

Received 25 May 2007; received in revised form 27 November 2007; accepted 6 December 2007
Available online 24 January 2008

Abstract

We have investigated three-dimensional (3-D) architectures – microspheres and radial structures – based on biopolymer-assisted self-assembly from one-dimensional ZnO nanorods. The developed method is simple, rapid and cost-effective and can be used for self-assembly of different complex superstructures. A possible model of 3-D architectures self-assembled with biopolymer assistance is presented using minimum energy considerations. Scanning electron microscopy, X-ray diffraction, energy dispersive X-ray spectroscopy, transmission electron microscopy, micro-Raman spectroscopy and cathode luminescence investigations show that the novel 3-D architectures are built from high-purity ZnO nanorods with a wurtzite structure. The resulting radial structures show an intense ultraviolet (UV) cathode luminescence emission suggesting applications as UV light emitting diodes or lasers. Their structural characteristics endow them with a broad area of applications and offer a possibility to be used as fundamental low-dimensional building units. These building units open opportunities for the self-assembly of multifunctional nanostructured systems with applications in bioscience and nanomedicine, electronics and photonics.

© 2007 Elsevier Ltd. All rights reserved.

Keywords: ZnO nanorod; Self-assembly; Nanofabrication; Cathodeluminescence

* Corresponding author at: Department of Microelectronics and Semiconductor Devices, Technical University of Moldova, 168 Stefan cel Mare Blvd., Chisinau, MD-2004, Republic of Moldova. Tel.: +373 (22) 509914; fax: +373 (22) 509910.

E-mail addresses: lupanoleg@yahoo.com, lupan@physics.ucf.edu (O. Lupan).

1. Introduction

Nanoarchitectures exhibit peculiar and fascinating properties distinct from their bulk counterparts due to the nanometric size structures and high surface area. For the self-assembly process it is important to synthesize different one-dimensional (1-D), two-dimensional (2-D), and three-dimensional (3-D) architectures. In nanofabrication, the control of the size, shape and arrangement of fundamental nanobuilding blocks is essential for cost-efficient, simple and effective preparation at low temperatures on any substrate. In this regard, the self-assembly method offers the possibility for individual components to interact in predefined ways that result in the spontaneous self-organization and integration into higher-order structures. Thus designing nanoarchitectures by self-assembly can be controlled using chemistry, which involves van der Waals forces, electrostatic forces, or hydrophobic interactions [1]. At the same time nanostructures are influenced by external forces, which provide flexibility for designers as electrostatic and hydrodynamic forces permit to guide processes [1,2].

The nanofabrication of functional ZnO architectures attracted special attention due to the novel effects of size, shape on their collective properties. The 1-D architectures such as nanowires, nanorods, nanotubes [2], and branched nanorods [3] are currently under intense research due to potential applications in nanodevices [4–6]. The next steps in this area of research will be the controlled assembly of 1-D nanorods, nanowires into 2-D or 3-D ordered structures [7] for concrete device application. Understanding and controlling the growth mechanism on the nanoscale is necessary to have high-quality nanobuilding blocks with tunable properties that will permit the assembly of superstructures for engineering of functional systems for specific purposes.

Nano-zinc oxide is a semiconductor material with various configuration architectures much richer than of any other known nanomaterial [2,10]. It is rapidly gaining in applicability for nanodevices [6,8,9]. ZnO has advantageous properties promising manifold applications [10] in ultraviolet (UV) lasers with low threshold [10–12], as hydrogen storage material [13], for field-emission displays [14], as UV-shielding material [15], for nanoscaled sensitive UV and gas sensors [16], for ultrasensitive DNA and bio-sensors in nanomedicine [17], etc. ZnO is an ideal candidate for fabricating UV light emitting diodes and lasers. ZnO is a phosphor material with the ability to retain a high efficiency and at low-voltage excitation [18]. Simple process techniques for arranging ZnO phosphor are necessary for widespread emission displays, with smaller size, higher resolution and better contrast compared to liquid crystal displays [19].

These benefits are motivation to progress various technological methods, and extensive efforts are made to control the assembly of ZnO nanoarchitectures with different morphologies and with different crystallographic forms and properties. However, most of the reported synthetic methods are limited to the growth of 1-D or 2-D ZnO (thin films) and only few on 3-D ordered architectures, which still remains a significant challenge. At the same time it is very difficult to self-assemble 1-D ZnO nanorods into 3-D complex superstructures [20,21] without understanding and controlling the different driving mechanisms [22,23] involved. 3-D ZnO microspheres and radial structures offer a possibility to study and control the growth mechanisms. These structures are of particular interest due to their lower densities and higher surface area [24,25], and the collective properties of assemblies of these nanorods are technologically relevant [1,26]. Hollow ZnO spheres have been fabricated by an integrated autoclave and pyrolysis process [27], by sacrificial template route [10], chemical vapour deposition (CVD) [28], and by a facile hydrothermal process on a compact TiO₂ substrate [29]. Self-assembly of ZnO spheres on interfaces in a Pickering emulsion has been performed by He et al. [30]. However,

these routes require the presynthesis of ZnO nanoparticles in a separate process. The self-assembly route to fabricate ZnO spheres and 3-D architectures has also been employed by using ZnCl_2 and $\text{Na}_2\text{C}_2\text{O}_4$ as precursors [7]. This method permits self-assembly of ZnO nanoplates into microspheres in 10 h at 180 °C [31]. However, these processes are time consuming and require more energy or complex set-ups [20] and will not keep the cost of manufacturing low.

The aqueous solution deposition from metal salts, on the other hand, is simple, cost-effective and permits coatings of differently shaped substrates. In addition it employs a low growth temperature (<100 °C) process compared to metal-organic CVD (>800 °C) and it has good potential for scale-up [32].

The aim of this study is to integrate 1-D ZnO nanorods as nanobuilding blocks into 3-D ZnO microspheres and radial structures through biopolymer-assisted self-assembly. Understanding and controlling the growing mechanisms is essential to self-assemble 3-D ZnO spheres and radial structures and to develop new technologies for self-assembly of novel nanodevices.

2. Experimental details

2.1. Synthesis

In this work a biopolymer-assisted self-assembly chemical route from aqueous solution has been used to grow and self-assemble 1-D nanorods into 3-D architectures. Glass or quartz substrates were cleaned using a procedure described in Ref. [33]. For silicon wafers, the procedure described in Ref. [34] was used to clean the substrate.

Zinc sulfate [$\text{Zn}(\text{SO}_4) \cdot 7\text{H}_2\text{O}$] and ammonia (NH_4OH) (Fisher Scientific, reagent grade, without further purification) were used for the synthesis of ZnO 3-D architectures. In a typical synthesis, 0.05–0.15 M $\text{Zn}(\text{SO}_4) \cdot 7\text{H}_2\text{O}$ and ammonia solution NH_4OH (29.6%) were mixed in 70 ml de-ionized water ($\sim 18.2 \text{ M } \Omega \text{ cm}$) until they were completely dissolved. In order to study the self-assembly of 1-D ZnO nanorods into 3-D superstructures, water-soluble biopolymer-sodium alginate (SA) 0.005–0.02 M was added to the complex solution in the growth reactor. The cleaned glass, quartz, and Si substrates were placed inside the aqueous solution in a specially designed reactor described in [3]. The setup was mounted onto a laboratory oven set to a temperature of 100 °C, and the reaction was allowed to proceed for different durations in the range 10–30 min without any stirring. In our experiments ZnO nanocrystals were formed at a pH value of 10–11. After a predetermined duration of the reaction at 100 °C and turning off the power, the whole system was left on the hot plate for 30 min to cool to 40 °C. Finally, the substrates were dipped and rinsed in deionized water for 2 min and then the samples were dried in air at 150 °C for 10 min.

2.2. Characterization

The crystal structures of the self-assembled ZnO 3-D-architectures were analyzed by X-ray diffraction (XRD) using a Rigaku 'D/B max' X-ray diffractometer equipped with a monochromatized $\text{Cu K}\alpha$ radiation source ($\lambda = 1.54178 \text{ \AA}$) and operating conditions of 30 mA and 40 kV at a scanning rate of 0.01 °/s in the 2θ scanning ranges from 10° to 90°. Data acquisition was made with Data Scan 3.1 and analysed with Jade 3.1 (from Materials Data Inc.). The composition and surface morphologies of ZnO films were studied with energy dispersion X-ray spectroscopy (EDX) and scanning electron microscopy (SEM) using a Hitachi S800. Transmission electron microscopy (TEM) was performed with a FEI Tecnai F30 TEM at an accelerating voltage of 300 kV.

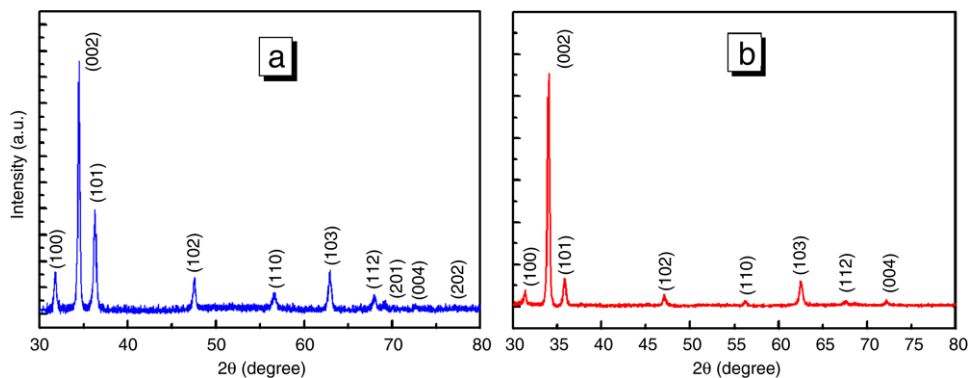


Fig. 1. XRD pattern of the ZnO nanorods: (a) microspheres; and (b) radial structures synthesized by the biopolymer-assisted self-assembly method. All diffraction peaks are indexed in agreement with the JCPDS 036-1451 card for ZnO.

With room-temperature micro-Raman spectroscopy the optical and structural properties of these ZnO structures were studied. Specimens were examined using micro-Raman scattering experiments with a Horiba Jobin Yvon LabRam IR system at a spatial resolution of 2 μm in backscattering configuration. The 633 nm line of a Helium Neon laser was used for off-resonance excitation with less than 4 mW of power at the sample. The spectral resolution was 2 cm^{-1} , and the instrument was calibrated to the same accuracy using a naphthalene standard. All Raman spectra were acquired at room temperature.

The cathodoluminescence (CL) spectroscopy measurements with high spatial resolution were carried out at room temperature using a Gatan MonoCL3 cathodoluminescence system, which is integrated with a Philips XL 30 Scanning Electron Microscope. The emitted radiation was analysed using a single grating (1200 lines/mm, blazed at 500 nm) and a Hamamatsu photomultiplier tube with sensitivity in the 185–850 nm range. An electron beam accelerating voltage of 10 kV was used, corresponding to an electron penetration depth of about 0.5 μm . The CL measurements were performed at room temperature.

3. Results and discussion

3.1. The structural characterization of ZnO nanoarchitectures

The phase purity and composition of the products obtained by the self-assembly method was examined by XRD and EDX. Fig. 1 shows the XRD results of 3D-architectures in the range of 30°–80° at a scanning step of 0.01°. All diffraction peaks are indexed according to the hexagonal phase of ZnO (wurtzite structure, space group: $P6_3mc(186)$; $a = 0.3249$ nm, $c = 0.5206$ nm) and the data are in agreement with the JCPDS 036-1451 card [35] for ZnO. No characteristic peaks of impurity phases such as Zn or S are observed and no diffraction peaks except ZnO are found. The intensity of the ZnO (002) peak is higher than that of bulk ZnO, indicating preferential growth along the c -axis in the [002] direction (Fig. 1) and good crystallinity of the samples.

Using energy dispersion X-ray spectroscopy, we found that the Zn:O ratios in our nanostructures to be 1:1 atomic ratio in all samples.

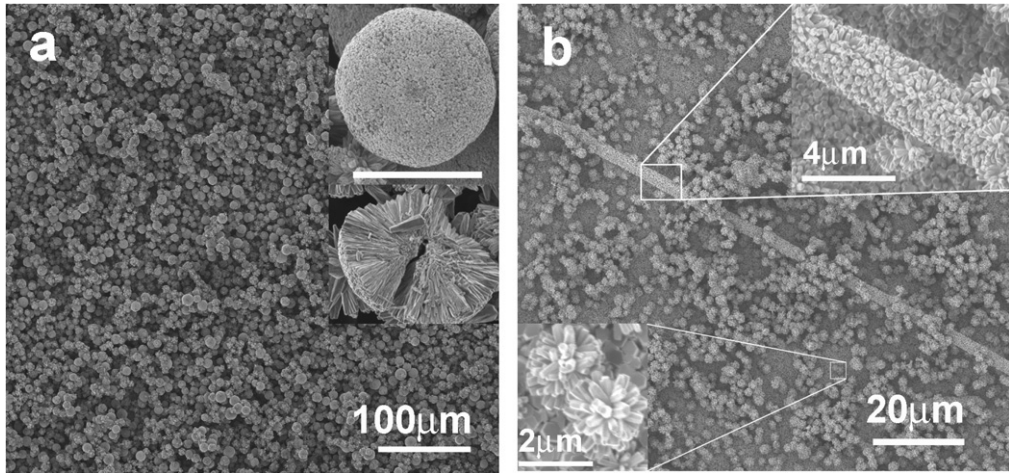


Fig. 2. Scanning electron micrographs of the ZnO architectures chemically grown by the biopolymer-assisted self-assembly method: (a) the overall morphology of ZnO nanorod-based microspheres. The insets are individual (up) and micromechanical broken microspheres (down), the scale bar in the inset is 10 μm ; (b) ZnO radial architectures from one-dimensional ZnO nanorods and insets with magnified images.

3.2. The morphology of the 3-D architectures

SEM has been used to examine the surface morphology and to estimate of the obtained structural sizes. Typical SEM micrographs of the ZnO architectures obtained by the biopolymer-assisted self-assembly method are shown in Fig. 2. Under the appropriate conditions as described in Section 2.1, it is possible to grow ZnO nanorod-based radial structures and microspheres using a biopolymer concentration in the range of 0.005–0.02 M and reaction duration from 10 to 30 min at 100 °C. The overall morphology of ZnO spheres with equal size on a Si substrate is shown in Fig. 2 (a), indicating that the 3-D architectures consist of 1-D nanorods with an average diameter of 100 nm (upper inset in Fig. 2(a)). From the insets in Fig. 2 (a) we can see that the ZnO nanorods are arranged in a perfectly spherical structure. The radii of ZnO nanorod-based spheres are around 5 μm after a reaction time of 30 min at 100 °C (see second inset in Fig. 2(a) of micromechanical broken “opened” microsphere). The nanorods occupy the entire volume in the spheres. New 3-D ZnO radial structures are presented in Fig. 2(b) obtained by the self-assembly method in 10 min at 100 °C using half of the concentration of the biopolymer compared to the previous sample shown in Fig. 2 (a). We investigate the possibility to control the self-assembly process of 1-D nanorods in 3D superstructures by different concentrations of organic biopolymers along with growth parameters. The inset SEM images in Fig. 2 clearly display 1-D hexagonal nanorods radially self-assembled in different 3-D architectures under biopolymer support.

Transmission electron microscopy was employed to characterize the as-synthesized ZnO nanorods, and to observe the nanostructures. To prepare TEM samples, they were transferred and mounted on the inside of a TEM Cu-grid by the in-situ lift-out technique in a Focused Ion Beam (FIB) system.

The corresponding TEM images and selected-area electron diffraction (SAED) pattern of the low-dimensional building block-ZnO nanorod are shown in Fig. 3. According to the inset with a

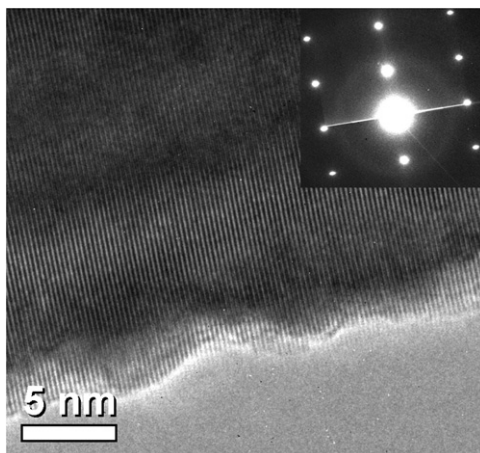


Fig. 3. The high-resolution TEM images and the inset with the selected-area diffraction pattern of the single-crystalline ZnO nanorods grown by self-assembly method.

SAED pattern (the up-right corner) in Fig. 3 the nanorod is grown along the [0001] direction of ZnO, which corresponds with the high-resolution TEM (HRTEM) result.

The TEM images indicate that the 1-D nanorod is single-crystalline ZnO with a wurtzite structure grown along the [0001] direction, which is consistent with the XRD results. The HRTEM lattice fringes and SAED patterns shown in Fig. 3 reveal that, in this region, the crystallographic [0001] axis is parallel to the long axis of the nanorod without dislocations and stacking faults. With TEM characterizations we found that 1-D nanorods are not bent, but have a smooth surface and therefore provide direct evidence for the orientated-attachment growth mechanism.

3.3. The proposed growth model and mechanism

According to our experimental results, a possible chemical mechanism for the reaction process and model for self-assembly of ZnO-nanorods into radial superstructures by biopolymer-assistance can be proposed as follows. Due to the fact that the heterogeneous nucleation takes place at a low level of supersaturation of the complex solution, we can grow different ZnO nanoarchitectures (Fig. 2) by controlling the reactant concentration, pH value, process temperature, and duration. Lowering the concentration of ammonia hydroxide permits the growth of smaller 1-D ZnO nanorods with radii less than 50 nm. At the same time by varying the concentration of long-chain biopolymer-SA in solution different radial superstructures are obtained (Fig. 2(a), (b)). Repeated experiments demonstrate that without biopolymer in the solution only ZnO nanorods can be obtained. The water-soluble long-chain biopolymer is the nucleation site for the self-assembly of radial structures and offers a possibility to control growth process for 3-D architectures.

The crystal synthesis on a biopolymer surface in the long-chain-assisted route is based on heterogeneous nucleation and subsequent growth. At the beginning, when the reactor is placed on a hot plate, the decomposition of the $\text{Zn}(\text{OH})_4^{2-}$ complex dissolves and leads to supersaturation beyond ZnO solubility. As the temperature increases the following reactions occur:



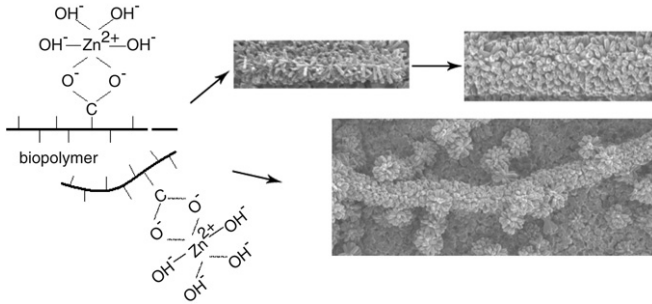
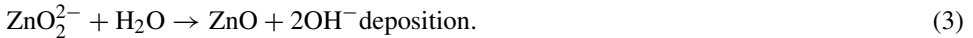


Fig. 4. Left: Representation of the proposed growing model and chemical mechanism for ZnO radial spherical structures build from nanorods under biopolymer-assisted self-assembly. Right: Corresponding SEM images of grown ZnO structures.



With an increase in temperature the $\text{Zn}(\text{OH})_4^{2-}$ ion decomposition takes place at the interface between biopolymer surface and solution and when the concentration of Zn^{2+} and OH^{-} exceed supersaturation, seeds form and ZnO crystals nucleate heterogeneously on the negatively charged biopolymer surface (see Fig. 4), and finally grow from the ZnO nucleus. A schematics of the electrostatic attraction between the Zn^{2+} and carboxylic groups within the negatively-charged biopolymer skeleton and SEM images of self-assembly radial structures are shown in Fig. 4. The nanostructures in solution attach to the surrounding bio-polymer and spontaneously cluster together into colloidal spherical aggregates to minimize their surface area [36]. At relatively high temperatures, oxygen atoms could coordinate with the neighbor complexes and cause self-assembly of 3-D ZnO architecture to condense. The nanorods, which tends to grow toward the exterior and radial growth, is physically limited due to of ZnO polar crystal growth. By the “lowest-energy” theory [37] that dictates the preferred growing direction, the 1-D nanorods growth mechanism can be explained.

The kinetic conditions in the nanorod formation during the self-assembling process, as shown in Fig. 4, may depend on the reagents’ concentrations, reaction temperature, pH value of the aqueous solution and different organic biopolymers added. Growth models of self-assembled hollow microspheres have been proposed and described in Refs. [20,36].

3.4. Micro-Raman scattering

An effective approach to investigate the phase and purity of the low-dimensional nanostructures is micro-Raman scattering. Room-temperature micro-Raman spectroscopy was performed to examine the properties of the self-assembly ZnO 3D structures. When considering ZnO, which has the wurtzite space group C_{6V}^4 , the phonon modes E_2 (low and high frequency), A_1 [(TO)-transverse optical and (LO)-longitudinal optical] and E_1 (TO and LO) are all expected to be Raman and infrared active. The eight optical phonons at the Γ point of the Brillouin zone belong to the schematics [38]:

$$\Gamma_{\text{opt}} = 1A_1 + 2B_1 + 1E_1 + 2E_2. \quad (4)$$

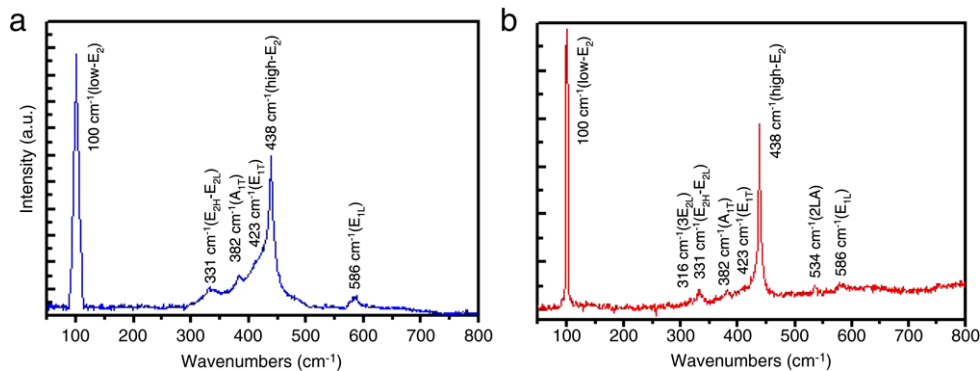


Fig. 5. Micro-Raman scattering spectra of the self-assembled ZnO nanorod-based: (a) microspheres; and (b) radial structures.

Representative micro-Raman spectra of the self-assembly ZnO nanorod-based spheres and radial spherical structures are shown in Fig. 5. Dominant peaks at 100 and 438 cm^{-1} , which are commonly detected in the wurtzite structure ZnO [39], are attributed to the low- and high- E_2 mode of nonpolar optical phonons, respectively. The weaker peak at 331 cm^{-1} has been attributed to a second order nonpolar E_2 mode [40], which is Raman active only and can be observed only when ZnO is single crystal. The Raman peak at 382 cm^{-1} originates from the polar A_1 mode of ZnO. The B_1 modes are infrared and Raman inactive (silent modes) [38]. The strong Raman peak at 438 cm^{-1} is one of the characteristic peaks of wurtzite ZnO attributed to the high frequency E_2 mode [41,42] assigned to multiple-phonon processes. According to the recorded Raman spectra the E_2 (high) is clearly visible at 438 cm^{-1} with a width of 10 cm^{-1} (Fig. 3(b)), indicating the good crystal quality [41,42] of the self-assembled radial structures. The E_1 (LO) mode near to 586 cm^{-1} is allowed in the $x(zz)x'$ scattering configuration and can be observed from the tilted nanorods (Fig. 5).

There are no significant differences between the measured spectra for differently shaped (straight and curved) 3-D nanorod-based radial structures both in spectral position or intensity.

3.5. Cathodeluminescence characterization

The room temperature cathode luminescence (CL) spectra of the self-assembly ZnO 3-D architectures were measured and are shown in Fig. 6. The CL emission spectrum of ZnO microspheres shows a broad band of emission covering the blue and green regions (Fig. 6(a)). This low-energy emission corresponds to the green band and could include several components usually associated to deep-level point defects — oxygen vacancies and zinc interstitials observed for ZnO films [43–45]. These spectra could reveal an inhomogeneous distribution of defects in the spheres. A similar CL spectrum for ZnO hollow microspheres was previously presented in Ref [20,46]. The origin of this emission still remains unclear, although it can be attributed to radiative defects.

The CL spectra of ZnO radial structures (Fig. 6(b)) reveal a strong and sharp UV emission at 389 nm, which corresponds to the near band edge emission of ZnO. The strong ultraviolet emission peak at 389 nm and a weak broad green emission band, suggest that the radial structures possess high crystal quality with minimum oxygen vacancies. Our results demonstrate that self-

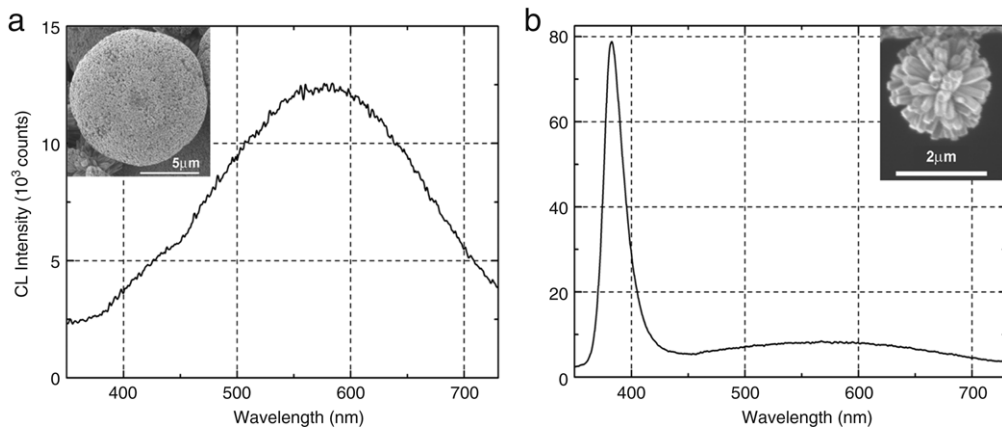


Fig. 6. Cathode luminescence (CL) spectra of the self-assembled one-dimensional ZnO nanorod-based: (a) microspheres, inset with the corresponding SEM image; and (b) radial spherical structures, inset with corresponding SEM image.

assembly of radial structures permits controlled growth of good quality nanostructures with few defects [27] for near-future optoelectronic nanodevices.

4. Conclusion

In summary, ZnO 3-D spheres and radial structures were synthesized through a novel, rapid, low-temperature, biopolymer-assisted self-assembly route without any template. The architectures are constructed of high-quality ZnO 1-D nanorods 100 nm in diameter and 2–5 μm in length.

X-ray diffraction, energy dispersive X-ray spectroscopy, scanning electron microscopy, transmission electron microscopy, micro-Raman spectroscopy, and cathode-luminescence (CL) measurements have been used to characterize the samples. These characterizations reveal that the ZnO 3-D architectures assemble from 1-D nanorods. These 1-D nanorods are found to have good crystal quality with *c*-axis orientation.

A possible model and growth mechanism of 3-D architectures during self-assembly under biopolymer assistance has been proposed on the basis of minimum energy theory.

The strength of the proposed nanotechnology is that any substrate can be used to rapidly grow ZnO nanorod-based 3-D radial spherical structures using biopolymer-assistance at low temperatures (100 °C). This offers the possibility to explore their novel collective properties and it could be further extended to assemble differently shaped architectures and tune their properties for specific device applications.

Due to the good crystallinity of the obtained products, room temperature CL spectra show an intensive and sharp UV emission at 389 nm for ZnO radial structures which confirm it to be an ideal candidate for fabricating ultraviolet light emitting diodes and lasers.

Further work on the optimization of pure and doped ZnO 1-D nanorod-based 3-D architectures may lead to an extension of the proposed cost-effective and efficient self-assembly technique for fabrication of nanoscale devices and nanosystem applications. It is anticipated that 3-D self-assembly will be used to explore new phenomena and materials behaviours in order to synthesize nanometer sized electronic and optoelectronic device in the near future.

Acknowledgements

The research described here was made possible in part by an award for young researchers (MTFP-1014B Follow-on) from the Moldovan Research and Development Association (MRDA) under funding from the US Civilian Research & Development Foundation (CRDF). Professor L. Chow acknowledges financial support from Apollo Technologies, Inc. and the Florida High Tech Corridor Research Program. Raman measurements were supported in part by NSF MRI grant DMR-0421253.

References

- [1] B. Amir Parviz, D. Ryan, G.M. Whitesides, *IEEE Trans. Adv. Packaging* 26 (2003) 233.
- [2] P.X. Gao, Zhong L. Wang, *J. Appl. Phys.* 97 (2005) 044304.
- [3] Oleg Lupan, Lee Chow, Guangyu Chai, Beatriz Roldan, Ahmed Naitabdi, Alfons Schulte, Helge Heinrich, Nanofabrication and characterization of ZnO nanorod arrays and branched microrods by aqueous solution route and rapid thermal processing, *Mater. Sci. Eng. B: Solid–State Mater. Adv. Technol.* 145 (2007) 57.
- [4] O. Lupan, G. Chai, L. Chow, Fabrication of ZnO nanorod-based hydrogen gas sensor, *Microelectron. J.* 38 (2007) 1211.
- [5] W.I. Park, J.S. Kim, G.C. Yi, H.-J. Lee, *Adv. Mater.* 17 (2005) 1393.
- [6] B.Z. Fan, J.G. Lu, Nanostructured ZnO: Building blocks for nanoscale devices, *Int. J. High Speed Electron. Syst.* 16 (4) (2006) 893.
- [7] H.X. Niu, Q. Yang, K.B. Tang, F. Yu, *J. Mater. Sci.* 41 (2006) 5784.
- [8] D.C. Look, B. Claflin, Ya.I. Alivov, S.J. Park, *Phys. Status Solidi A* 201 (10) (2004) 2203.
- [9] E. Tang, G. Cheng, X. Pang, X. Ma, F. Xing, *Colloid Polym Sci.* 284/4 (2006) 422.
- [10] Ü. Özgür, Ya.I. Alivov, C. Liu, A. Teke, M.A. Reshchikov, S. Dogan, V. Avrutin, S.J. Cho, H. Morkoç, Comprehensive review of ZnO materials and devices, *J. Appl. Phys.* 98 (2005) 041301.
- [11] S.F. Yu, Yuen Clement, S.P. Lau, W.I. Park, Yi Gyu-Chul, *Appl. Phys. Lett.* 84 (17) (2004) 3241.
- [12] M.H. Huang, S. Mao, H. Feick, H. Yan, H. Kind, E. Weber, R. Russo, P. Yang, *Science* 287 (2000) 465.
- [13] H. Pan, J. Luo, H. Sun, Y. Feng, C. Poh, J. Lin, *Nanotechnology* 17 (2006) 2963.
- [14] Z. Fan, J.G. Lu, *J. Nanosci. Nanotechnol.* 5 (2005) 1561.
- [15] M.N. Xiong, G.X. Gu, B. You, L.M. Wu, *J. Appl. Polym. Sci.* 90 (2003) 1923; Yuan-Qing Li, Shao-Yun Fu, Yiu-Wing Mai, *Polymer* 47 (6) (2006) 2127.
- [16] Z. Fan, J.G. Lu, *IEEE Trans. Nanotechnol.* 5 (4) (2006) 393.
- [17] N. Kumar, A. Dorfman, J. Hahm, *Nanotechnology* 17 (2006) 2875.
- [18] K. Morimoto, in: S. Shionoya, W.M. Yen (Eds.), *Phosphor Handbook*, CRC Press, Boca Raton, FL, 1998 (Chapter 8).
- [19] N. Saito, H. Haneda, T. Sekiguchi, N. Ohashi, I. Sakaguchi, K. Koumoto, *Adv. Mater.* 14 (6) (2002) 418.
- [20] S. Gao, H. Zhang, X. Wang, R. Deng, D. Sun, G. Zheng, *J. Phys. Chem.* 110 (2006) 15847.
- [21] M. Mo, J.C. Yu, L. Zhang, S.-K.A. Li, *Adv. Mater.* 17 (2005) 756; Challa S.S.R. Kumar, Josef Hormes, Carola Leuschner, *Nanofabrication Towards Biomedical Applications*, Wiley-VCH Verlag GmbH & Co. KGaA, 2005, *Nanostructured Systems from Low-Dimensional Building Blocks* Chapter Authors: Donghai Wang, Maria P. Gil, Guang Lu, Yunfeng Lu.
- [22] H. Wang, C. Xie, D. Zeng, Z. Yang, *J. Colloid. Interface Sci.* 297 (2006) 570.
- [23] J.S. Jeong, J.Y. Lee, J.H. Cho, H.J. Suh, C.J. Lee, *J. Chem. Mater.* 17 (10) (2005) 2752.
- [24] H. Jin Fan, Roland Scholz, F.M. Kolb, M. Zacharias, U. Gösele, *Solid State Commun.* 130 (2004) 517.
- [25] S. Ding, J. Guo, X. Yan, T. Lin, K. Xuan, *J. Cryst. Growth* 284 (2005) 142.
- [26] M.P. Pileni, *J. Phys. Chem. B* 105 (2001) 3358.
- [27] J. Duan, X. Huang, E. Wang, H. Ai, *Nanotechnology* 17 (2006) 1786.
- [28] J.J. Wu, S.C. Liu, *Adv. Mater.* 14 (3) (2002) 215.
- [29] L. Shi, X. Sun, H. Li, D. Weng, *Mater. Lett.* 60 (2) (2006) 210.
- [30] Y. He, *Mater. Lett.* 59 (2005) 114.
- [31] Y. Peng, An-Wu Xu, B. Deng, M. Antonietti, H. Cölfen, *J. Phys. Chem. B* 110 (2006) 2988.
- [32] Yee Wee Koh, Kian Ping Loh, *J. Mater. Chem.* 15 (2005) 2508.
- [33] S.T. Shishiyau, O.I. Lupan, E.V. Monaico, V.V. Ursaki, T.S. Shishiyau, I.M. Tiginyanu, *Thin Solid Films* 488 (2005) 15.

- [34] S.T. Shishiyanu, O.I. Lupan, T.S. Shishiyanu, V.P. Şontea, S.K. Railean, *Electrochim. Acta* 49 (25) (2004) 4433.
- [35] Joint Committee on Powder Diffraction Standards, Powder Diffraction File No 36-1451.
- [36] M. Mo, J.C. Yu, L. Zhang, S.-K.A. Li, *Adv. Mater.* 17 (6) (2005) 756.
- [37] L. Guo, Y.L. Ji, H. Xu, *J. Am. Chem. Soc.* 124 (2002) 14864.
- [38] C. Bundesmann, N. Ashkenov, M. Schubert, D. Spemann, T. Butz, E.M. Kaidashev, M. Lorenz, M. Grundmann, *Appl. Phys. Lett.* 83 (2003) 1974.
- [39] Y.J. Xing, Z.H. Xi, Z.Q. Xue, X.D. Zhang, J.H. Song, R.M. Wang, J. Xu, Y. Song, S.L. Zhang, D.P. Yu, *Appl. Phys. Lett.* 83 (2003) 1689.
- [40] J.M. Calleja, M. Cardona, *Phys. Rev. B* 16 (1977) 3753.
- [41] T.C. Damen, S.P.S. Porto, B. Tell, *Phys. Rev.* 142 (1966) 570.
- [42] Z. Li, Y. Xiong, Y. Xie, *Nanotechnology* 16 (2005) 2303.
- [43] W.L. Schaich, N.W. Ashcroft, *Solid State Commun.* 8 (23) (1970) 1959.
- [44] R.T. Cox, D. Block, A. Herve, R. Picard, C. Santier, R. Helbig, *Solid State Commun.* 25 (2) (1978) 77.
- [45] N.O. Korsunskaya, L.V. Borkovskaya, B.M. Bulakh, L.Yu. Khomenkova, V.I. Kushnirenko, I.V. Markevich, *J. Lumin.* 102–103 (2003) 733.
- [46] L. Khomenkova, P. Fernandez, J. Piqueras, *Cryst. Growth Design* 7 (4) (2007) 836.